

BAD Phosphorylation Determines Ovarian Cancer Chemosensitivity and Patient Survival

Douglas C. Marchion^{1,2}, Hope M. Cottrill¹, Yin Xiong^{1,2}, Ning Chen^{1,2}, Elona Bicaku^{1,2}, William J. Fulp³, Nisha Bansal¹, Hye Sook Chon¹, Xiaomang B. Stickles¹, Siddharth G. Kamath^{1,4}, Ardeshir Hakam⁵, Lihua Li⁸, Dan Su⁹, Carolina Moreno², Patricia L. Judson^{1,2}, Andrew Berchuck¹⁰, Robert M. Wenham^{1,2}, Sachin M. Apte¹, Jesus Gonzalez-Bosquet^{1,7}, Gregory C. Bloom⁴, Steven A. Eschrich⁴, Said Sebt⁶, Dung-Tsa Chen³, and Johnathan M. Lancaster^{1,2}

Abstract

Purpose: Despite initial sensitivity to chemotherapy, ovarian cancers (OVCA) often develop drug resistance, which limits patient survival. Using specimens and/or genomic data from 289 patients and a panel of cancer cell lines, we explored genome-wide expression changes that underlie the evolution of OVCA chemoresistance and characterized the BCL2 antagonist of cell death (BAD) apoptosis pathway as a determinant of chemosensitivity and patient survival.

Experimental Design: Serial OVCA cell cisplatin treatments were performed in parallel with measurements of genome-wide expression changes. Pathway analysis was carried out on genes associated with increasing cisplatin resistance (EC_{50}). BAD-pathway expression and BAD protein phosphorylation were evaluated in patient samples and cell lines as determinants of chemosensitivity and/or clinical outcome and as therapeutic targets.

Results: Induced *in vitro* OVCA cisplatin resistance was associated with BAD-pathway expression ($P < 0.001$). In OVCA cell lines and primary specimens, BAD protein phosphorylation was associated with platinum resistance ($n = 147, P < 0.0001$) and also with overall patient survival ($n = 134, P = 0.0007$). Targeted modulation of BAD-phosphorylation levels influenced cisplatin sensitivity. A 47-gene BAD-pathway score was associated with *in vitro* phosphorylated BAD levels and with survival in 142 patients with advanced-stage (III/IV) serous OVCA. Integration of BAD-phosphorylation or BAD-pathway score with OVCA surgical cytoreductive status was significantly associated with overall survival by log-rank test ($P = 0.004$ and $P < 0.0001$, respectively).

Conclusion: The BAD apoptosis pathway influences OVCA chemosensitivity and overall survival, likely via modulation of BAD phosphorylation. The pathway has clinical relevance as a biomarker of therapeutic response, patient survival, and as a promising therapeutic target. *Clin Cancer Res*; 17(19); 6356–66. ©2011 AACR.

Introduction

The development of chemoresistance dramatically affects survival for patients with ovarian cancer (OVCA);

Authors' Affiliations: ¹Department of Women's Oncology, ²Experimental Therapeutics Program, ³Biostatistics Core, ⁴Bioinformatics Core, ⁵Department of Anatomic Pathology, and ⁶Drug Discovery Program, H. Lee Moffitt Cancer Center and Research Institute; ⁷James A. Haley Veterans' Hospital, Tampa, Florida; ⁸College of Life Information Sciences and Instrument Engineering, Hangzhou Dianzi University; ⁹Zhejiang Cancer Hospital, Hangzhou, China; and ¹⁰Department of Obstetrics and Gynecology/Division of Gynecologic Oncology, Duke University, Durham, North Carolina

Note: Supplementary data for this article are available at Clinical Cancer Research Online (<http://clincancerres.aacrjournals.org/>).

Corresponding Author: Johnathan M. Lancaster, Moffitt Cancer Center, 12902 Magnolia Drive, MCC-GYNPROG, Tampa, FL 33647. Phone: 813-745-4734; Fax: 813-745-4801; E-mail: johnathan.lancaster@moffitt.org

doi: 10.1158/1078-0432.CCR-11-0735

©2011 American Association for Cancer Research.

thus, targeted therapies that increase chemosensitivity offer the potential to significantly improve outcome. Although most patients with OVCA show remarkable sensitivity to platinum-based chemotherapy during primary therapy, these patients eventually develop platinum-resistant, recurrent disease (1, 2). Once platinum resistance has developed, few active therapeutic options exist, and patient survival is generally short lived (3). In this context, platinum resistance is frequently viewed as a surrogate clinical marker for more generic chemoresistance, and defining the molecular changes that drive the evolution of the platinum-resistant phenotype could contribute to a broader understanding of human cancer chemoresistance. Changes in cellular drug efflux, increased cellular glutathione levels, increased DNA repair, and drug tolerance have all been shown to contribute to platinum resistance (4–6). More recently, genomic studies have defined gene expression signatures that may discriminate between cancers that

Translational Relevance

Despite initial sensitivity to chemotherapy, patients with ovarian cancer (OVCA) often develop drug resistance, which limits survival. In this study, we explored genome-wide expression changes that underlie the evolution of chemoresistance and characterized the BCL2 antagonist of cell death (BAD) apoptosis pathway as a determinant of chemosensitivity and patient survival. Expression of the BAD pathway and also BAD protein phosphorylation status was associated with *in vitro* and *in vivo* platinum resistance, as well as overall survival, in more than 140 patients with advanced-stage (III/IV) serous OVCA, independent of surgical cytoreductive status. The BAD apoptosis pathway influences OVCA chemosensitivity and overall survival, likely via modulation of BAD phosphorylation. The pathway has clinical relevance as a biomarker of therapeutic response and patient survival, and as a promising therapeutic target.

are innately chemosensitive versus those that are chemoresistant (7–9). However, the genome-wide expression changes associated with the transition of an OVCA cell from chemosensitive to chemoresistant are less clear, and the discrete biologic pathways that drive the process are unknown. Moreover, how these pathways influence clinical outcomes and their potential as therapeutic targets remain to be defined.

In this study, we tracked the genome-wide expression changes associated with the evolution of *in vitro* cisplatin resistance. In doing so, we identified a pathway that seems to have a pivotal and wide-ranging influence on human cancer chemosensitivity, likely via phosphorylation of a key apoptotic protein. We evaluated the BCL2 antagonist of cell death (BAD) apoptosis pathway and phosphoprotein in OVCA cell lines and patient samples/data sets (i) as a potential biomarker of chemotherapy response and overall survival and (ii) as a therapeutic target to reverse OVCA chemoresistance.

Materials and Methods

Overview

A panel of OVCA cell lines was subjected to serial cisplatin treatment, and induced cisplatin resistance was quantified. In parallel, genome-wide expression changes were measured, and genes with expression correlating with increasing cisplatin resistance were analyzed for representation of biologic pathways. In light of the association between cisplatin resistance and expression of BAD-pathway kinases and phosphatases, we measured levels of phosphorylated BAD (pBAD) protein in both treated cell lines and chemosensitive and chemoresistant OVCA patient samples. BAD phosphorylation status was modified *in vitro* by using targeted siRNA and phosphorylation-site mutagenesis strategies, and the impact on cisplatin sensi-

tivity was measured. Expression of the BAD pathway was studied in a range of cancer cell types, and the influence on sensitivity to a variety of chemotherapeutics was measured. Finally, a BAD-pathway expression signature was developed and evaluated in treated cell lines and in patient data sets. To execute these analyses, 3 sample/data sets were used: (i) a panel of 8 cell lines, which were subjected to serial cisplatin treatments; (ii) genome-wide expression data from 142 patients treated at Duke University Medical Center and Moffitt Cancer Center (MCC), including 114 previously reported(8) and 28 new samples; and (iii) 147 OVCA samples obtained from the University of Minnesota (UMN, $n = 49$) and MCC ($n = 98$) and analyzed by immunofluorescence for phospho-BAD protein levels. As such, this study included analysis of data/specimens from 289 (142 + 147) OVCA patients treated at MCC, Duke, and UMN.

Induction of *in vitro* platinum resistance

The OVCA cell lines—A2008, A2780CP, A2780S, C13, IGROV1, OV2008, OVCAR5, and T8—were provided by Dr. Patricia Kruk (Department of Pathology, College of Medicine, University of South Florida, Tampa, FL) and maintained as previously described (ref. 10; Supplementary Data). Of note, C13 is a cisplatin derivative of OV2008, and T8 is a topotecan-resistant subclone of IGROV1. Such paired sensitive/resistant cell lines were included in the analysis to ensure that we were able to identify genomic changes associated with increased cisplatin resistance from a variety of baseline sensitivity/resistance states. Cells were subjected to sequential treatment with increasing doses of *cis*-diammine-dichloroplatinum (cisplatin), using 3 dosing schedules resulting in 144 treatment/expansion cycles (Supplementary Fig. S1). Treatment schedules A, B, and C included 3 treatments with 1, 2, and 3 $\mu\text{g}/\text{mL}$ cisplatin, respectively, followed by 3 treatments with 3, 4, and 5 $\mu\text{g}/\text{mL}$, respectively. Each cisplatin treatment was followed by a cell recovery/expansion phase. Both cisplatin resistance and genome-wide expression changes were measured serially in each cell line at baseline and after 3 and 6 cisplatin-treatment/expansion cycles. We quantified cisplatin resistance by using CellTiter-96 MTS proliferation assays (Fisher Scientific) and analyzed genome-wide expression by using Affymetrix Human U133 Plus 2.0 GeneChips as previously described [refs. 10, 11; Gene Expression Omnibus (GEO) accession number GSE23553]. Mycoplasma testing was done on the cell lines every 6 months following the manufacturer's protocol (Stratagene).

Statistical analysis of cell line array data

Pearson correlation was used to identify genes associated with OVCA development of cisplatin resistance (EC_{50}). Expression was calculated by using the robust multiarray average algorithm (12) implemented in Bioconductor (<http://www.bioconductor.org>) extensions to the R-statistical programming environment as described previously (13). Probe sets with expression ranges less than 2-fold

(maximum/minimum) and control probes (i.e., AFFX_* probe sets) were excluded from the analysis. For each cell line, Pearson correlation coefficients were calculated for expression data and cisplatin EC₅₀ (Supplementary Table S1). Genes/probe sets showing expression/EC₅₀ correlations ($|R| > 0.85$) were subjected to biological pathway analysis, using GeneGo/MetaCore software (Supplementary Table S2). Maps/pathways were identified by using the GeneGo/MetaCore statistical test for significance ($P < 0.001$).

Primary OVCA patient samples

OVCA samples/data sets from 289 patients treated at MCC, Duke, and UMN were analyzed in this study, including (1) genome-wide expression data from 142 patients treated at Duke and MCC [including 114, previously reported (8) and 28 new samples] and (2) 147 OVCA samples obtained from UMN ($n = 49$) and MCC ($n = 98$) and analyzed by immunofluorescence for pBAD protein levels. In brief, all 289 patients were known to have advanced-stage (III/IV), serous epithelial OVCA and underwent primary cytoreductive surgery followed by primary therapy with a platinum-based regimen (with or without taxane or cyclophosphamide). Additional details are provided in the Supplementary Data.

Statistical analysis of primary OVCA genomic data

Probe sets differentially expressed between primary platinum therapy complete responder (CR; $n = 101$) and incomplete responder (IR; $n = 41$) OVCA samples were identified by Student's t test ($P < 0.01$) and subjected to GeneGo/MetaCore pathway analysis.

Characterization of the BAD apoptosis pathway proteins in primary OVCA cell lines

Total BAD, pBAD (serine-112, -136, -155), nonphosphorylated BAD (Genscript), and BAD phosphatase PP2C/PPM1A (Santa Cruz Biotechnology) protein levels were evaluated in a subset of the cell line panel (8 cisplatin-treated OVCA cell lines) and in primary OVCA samples by Western blot or by immunofluorescence as previously described (14, 15).

Western blot analysis

Cells were harvested in media by using a Cell Lifter, washed with cold PBS, and solubilized by using SDS lysis buffer [2% SDS, 10% glycerol, 0.06 mol/L Tris (pH 6.8)]. The resultant lysate (50 μ g) was immediately separated on SDS-PAGE gels and transferred to nitrocellulose membranes. Membranes were blocked in Tris-buffered saline containing 0.05% Tween 20 (TBST)-5% nonfat milk and incubated with primary antibody in TBST-5% nonfat milk overnight at 4°C. Membranes were washed 3 times for 5 minutes with TBST and incubated with the appropriate secondary antibody in TBST-5% nonfat milk for 90 minutes at room temperature. Membranes were again washed 3 times for 5 minutes with TBST, and antibody binding was visualized by chemiluminescence on autoradiography film.

Immunofluorescence microscopy

Slides were deparaffinized and rehydrated by using xylene followed by serial dilutions of ethanol and subjected to heat-induced epitope retrieval by incubation in Tris-EDTA buffer [10 mmol/L Tris base, 1 nmol/L EDTA, 0.05% Tween 20 (pH 9.0)] for 20 minutes at 100°C. Slides were washed in PBS, incubated in blocking serum (0.3% Triton X-100, 0.1% normal goat serum in PBS) for 1 hour at room temperature, and exposed to primary antibody in blocking serum for 48 hours at 4°C. Slides were washed 3 \times in PBS, incubated with fluorescent-labeled secondary antibody in blocking serum for 2 hours at room temperature, and counterstained and mounted with Prolong Gold containing 4',6-diamidino-2-phenylindole (DAPI; Invitrogen). Images were acquired as TIFF files by using the Zeiss Axio Imager Z1 automated fluorescent scope and analyzed for percent expressing cells by Image Pro Plus software.

siRNA transfection

RNA duplexes for PP2C/PPM1A (s10909 and s10919; ABI), cAMP-dependent protein kinase (PKA; 6406 and 6574; Cell Signaling), and pFlag-600 vectors containing full-length BAD harboring serine (S) to alanine (A) mutations of the individual phosphorylation sites (S112A, S136A, S155A; kind gifts from Dr. Hong Gang Wang, MCC) were transfected by the Nucleofector transfection kit, according to the manufacturer's protocols (Amaxa). Briefly, cells (4×10^6) were suspended in 0.1 mL electroporation buffer V containing 1 μ mol/L siRNA and pulsed once by using program X-001. Pulsed cells were resuspended in 0.5 mL of complete media without antibiotics and incubated at 37°C for 15 minutes before experimentation. The *Silencer* negative control no. 2 siRNA (4390846; ABI), a nontargeting siRNA duplex, was used as a control. MTS cell viability analyses (CellTiter96; Promega) were used to evaluate cellular proliferation rate at 72 hours for cells expressing wild-type, S112A, S136A, and S155A mutations.

Analysis of apoptotic nuclei

Morphologic assessment of condensed chromatin and fragmented DNA was used to quantify percent apoptotic nuclei. Cells were fixed in 4% paraformaldehyde, and nuclei were stained with bis-benzimide trihydrochloride (0.5 μ g/mL; Molecular Probes) and quantified by fluorescence microscopy (15).

Evaluation of BAD-pathway genes

The BAD-pathway score was computed in the panel of OVCA cells previously subjected to serial cisplatin treatment. It was also independently computed for the clinical-genomic OVCA data set ($n = 142$ OVCA samples from MCC and Duke). For the cell line data, Pearson correlation was used to test any linear relationship between the BAD-pathway score derived from the cell line data and levels of pBAD proteins. For the clinical-genomic OVCA data set, log-rank test with Kaplan–Meier survival curves was used to test whether the median-split BAD-pathway score derived from the OVCA patient data was associated with overall survival.

Specifically, using genomic data from the panel of OVCA cells previously subjected to serial cisplatin treatment, principal component analysis was used to derive a BAD-pathway gene expression signature with a corresponding "pathway score" that represents overall gene expression levels for BAD-pathway genes. The generation of the signature used data from cell lines only; no patient data were used. Details of the statistical methodology used to generate the BAD-pathway gene expression signature are provided in the Supplementary Data. Briefly, as outlined above, using the GeneGo/MetaCore statistical test for significance, analysis of gene expression/EC₅₀ data from for the panel of OVCA carcinoma *in situ* (CIS)-treated cell lines, identified the BAD apoptosis pathway ($P < 0.001$) to be associated with cell line CIS resistance. GeneGo/MetaCore-defined objects (genes) within the BAD pathway, associated with OVCA cell line CIS EC₅₀, were thus identified. All probe sets, for each BAD pathway object identified in this way, were selected for inclusion in generation of the principal component analysis score. These 98 probe sets represented 47 genes. For this cell line data, Pearson correlation was used to test any linear relationship between the BAD-pathway score derived from the cell lines and levels of pBAD proteins. The BAD-pathway gene expression signature score developed in OVCA cell lines was evaluated in an independent set of 142 MCC/Duke OVCA samples. For this clinical-genomic OVCA data set, log-rank test with Kaplan–Meier survival curves were used to test any association between the BAD-pathway score ("high" vs. "low" on the basis of a median value cutoff) and overall survival for patients with OVCA. No data from the 142 MCC/Duke OVCA samples were used to identify the 47-gene signature; the MCC/Duke ovarian data were a completely independent evaluation set.

Results

Expression of BAD-pathway genes correlates with the evolution of platinum resistance

In the OVCA cell lines that we subjected to serial cisplatin treatment, expression of 3,111 unique probe sets, representing 2,434 unique genes, correlated across dose levels with cisplatin resistance, as measured by EC₅₀ (Pearson correlation coefficient > 0.85 , absolute value). GeneGO MetaCore analysis identified the "BAD phosphorylation, apoptosis and survival" pathway to be associated with development of *in vitro* cisplatin resistance ($P < 0.001$; Fig. 1). This BAD pathway includes 47 genes (98 probe sets in Affymetrix 133A chip; Supplementary Table S3), which were used to derive a BAD-pathway score in the cell line data and the OVCA patient samples. Statistical significance was derived from the number of genes that were input into the analysis software, the number of input genes present in a specific pathway, and the actual number of genes in that pathway. Thus, the P value represents the probability that mapping a set of genes to a particular pathway occurs by chance. BAD-pathway genes found to be associated with the evolution of *in vitro* cisplatin resis-

tance included *BAD*, *Bax*, *Bcl-XL*, *PP2C/PPM1A*, *AKT*, *EGFR*, *IRS-1*, *Shc*, *H-Ras*, *CDK1*, *G-protein alpha-s*, *G-protein beta/gamma*, *PI3K cat class 1A*, *c-Raf-1*, *p90Rsk*, *MEK2 (MAP2K2)*, *PKA-cat*, and *PKA-reg* (Fig. 1).

Genes associated with patient OVCA platinum response

In 142 OVCA patient samples, 397 probe sets, representing 347 unique genes, were identified as differentially expressed ($P < 0.01$) between CR and IR primary OVCAs (Supplementary Table S2). Pathway analysis of these 347 unique genes showed representation of the "BAD-phosphorylation, apoptosis and survival" pathway to be approaching statistical significance ($P < 0.08$). Analysis of IR versus CR ($P < 0.05$ threshold) for patients subjected to optimal versus suboptimal surgical cytoreduction showed representation of the BAD pathway at a statistically significant level ($P = 0.004$ and $P < 0.001$, respectively).

BAD protein phosphorylation status is associated with *in vitro* and *in vivo* chemoresistance and overall survival

Many of the BAD-pathway genes found to be associated with evolution of *in vitro* cisplatin resistance are known to influence BAD phosphorylation (Fig. 1). We therefore, tested the hypothesis that BAD protein phosphorylation status is associated with OVCA cisplatin resistance. Protein levels of total BAD, pBAD (serine-112, -136, and -155), total BAD protein, the BAD phosphatase PP2C/PPM1A, the phosphorylated form of the BAD kinase PKA, and total PKA protein were evaluated by Western blot analysis or immunofluorescence in (i) OVCA cell lines subjected to serial cisplatin treatment (T8) and/or (ii) 147 primary OVCA samples (MCC/UIMN; Fig. 2).

OVCA cell lines subjected to *in vitro* cisplatin-treatment/expansion cycles

Serially treated OVCA cells showed higher cisplatin EC₅₀ values and corresponding overall higher levels of both pBAD (serine-112, -136, -155) and pPKA than before serial cisplatin treatment (Fig. 2A). In contrast, protein levels of the BAD phosphatase PP2C/PPM1A were expressed at lower levels in serially cisplatin-treated cells.

Primary OVCA samples

Consistently, analysis of 147 patient primary OVCAs revealed higher levels of pBAD (serine-112, -136, and -155) in platinum-resistant (IR) than in platinum-sensitive (CR) samples ($P < 0.001$, $P = 0.02$, and $P < 0.001$, respectively; Fig. 2B). Immunofluorescence data were available for 134 of 147 samples for analysis of serine-112, 134 of 147 for serine-136, and 137 of 147 for serine-155. Median level of pBAD of each serine was used to as a cutoff to dichotomize patients into 2 groups, high versus low level of pBAD. Log-rank test with Kaplan–Meier survival curves revealed that patients with low levels of serine-112 had superior survival versus patients with high levels of pBAD ($P = 0.001$; Fig. 3A).

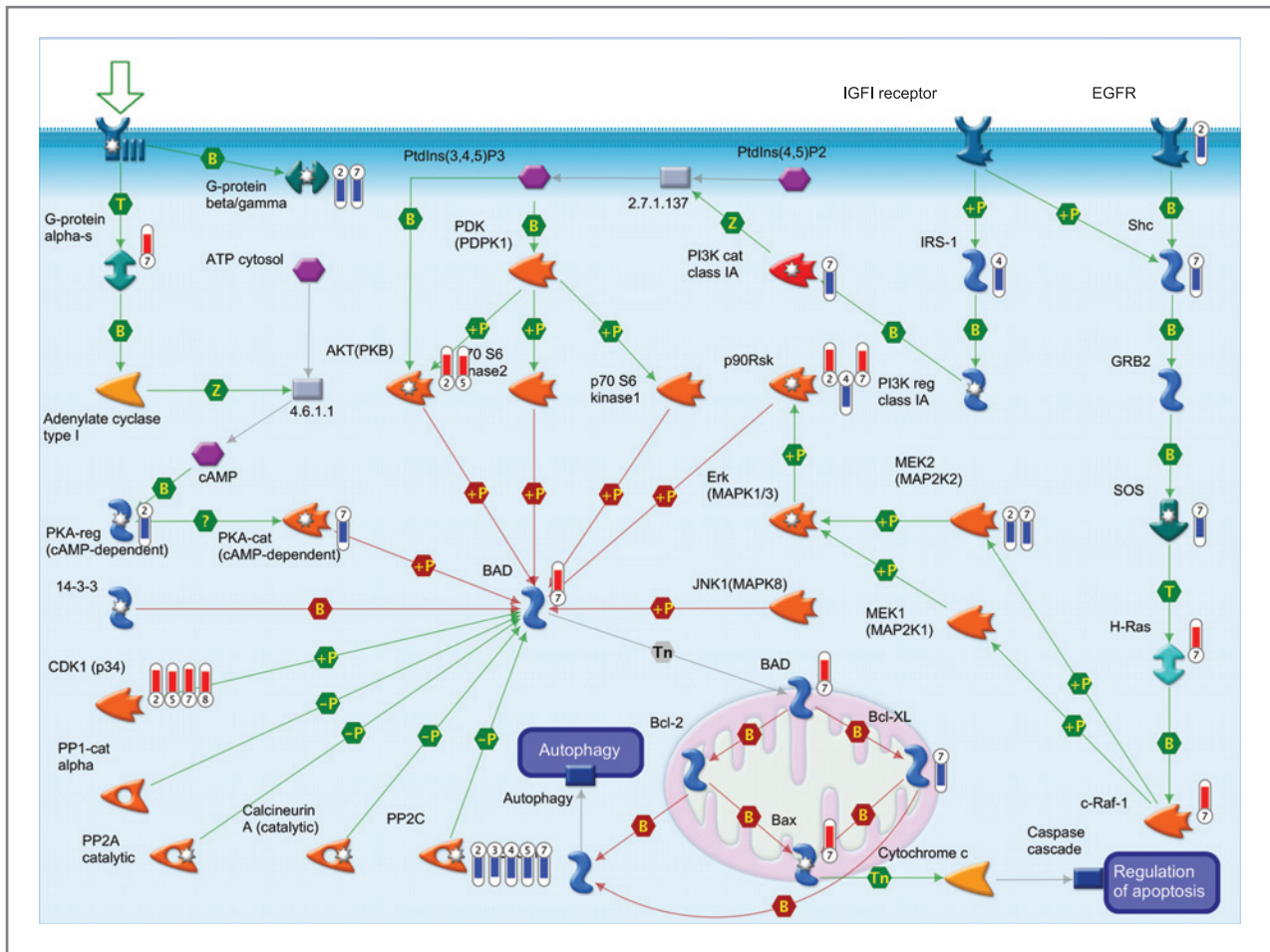


Figure 1. BAD pathway in genes associated with induced cisplatin resistance. Thermometers indicate those genes with positive (upward pointing) and negative (downward pointing) correlations between expression and increased cisplatin resistance (EC_{50} ; $P < 0.001$ for pathway enrichment); upward pointing thermometers identify genes with increasing expression associated with increasing OVCA cisplatin resistance, and downward pointing thermometers identify genes with decreasing expression associated with increasing OVCA cisplatin resistance. Numbers 1 to 8 at base identify the cell line (1, T8; 2, OVCAR5; 3, OV2008; 4, IGROV1; 5, C13; 6, A2780S; 7, A2780CP; 8, A2008) showing changes in expression of that gene with increasing cisplatin resistance. EGFR, epidermal growth factor receptor; IGF1, insulin like growth factor I.

Integration of the median-cut-off pBAD (serine-112) with the cytoreductive surgery (optimal vs. suboptimal) showed significant association with overall survival ($P = 0.004$ by log-rank test; Fig. 3B). Specifically, patients who had optimal cytoreductive surgery with low levels of pBAD (serine-112) had superior survival versus patients who had optimal cytoreductive surgery with high levels of pBAD [adjusted $P = 0.03$ by Holm method (16; Fig. 3B)]. Although it was not statistically significant, the same trend was observed for patients who had suboptimal cytoreductive surgery with low pBAD (serine-112) levels versus patients who had suboptimal debulking with high pBAD (serine-112) levels (adjusted $P = 1$). Similarly, patients who had suboptimal cytoreductive surgery with low pBAD (serine-112) had survival that trended toward superiority, but was not statistically significant, compared with patients who had optimal cytoreductive surgery with high levels of pBAD (adjusted $P = 1$; Fig. 3B). Patients who had subop-

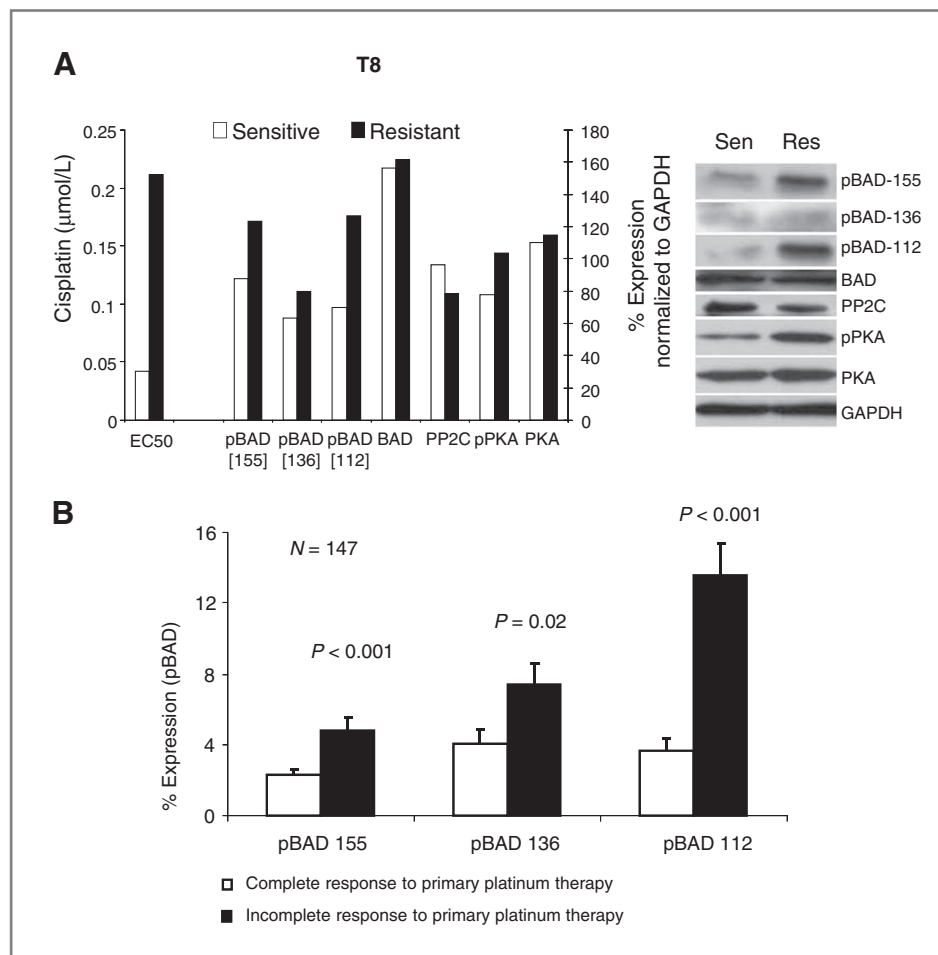
timal cytoreductive surgery with high levels of pBAD (serine-112) had the poorest overall survival (Fig. 3B). Serine-136 and -155 levels were not associated with overall survival. Although log-rank test with Kaplan–Meier survival curves revealed no statistically significant differences in survival on the basis of levels of pBAD serine-136 ($P = 0.40$) or pBAD serine-155 ($P = 0.43$), patients with high versus low levels of pBAD at both of these phosphorylation sites were observed to have lower median survival, although differences did not reach statistical significance ($P = 0.6$ and 0.2 , respectively; Fig. 3C and D).

Direct and indirect modulation of BAD phosphorylation status

Modulation of BAD phosphorylation status influenced cisplatin sensitivity in OVCA cell lines. Overrepresentation of nonphosphorylated BAD by transfection of A2780S and A2780CP cells with vectors containing serine (S) to alanine

Downloaded from http://aacrjournals.org/clinccancerres/article-pdf/17/19/6356/2000135/6356.pdf by guest on 25 June 2024

Figure 2. BAD protein phosphorylation is associated with platinum resistance. **A**, comparison of cisplatin EC₅₀ as determined by MTS cell viability assays and percent expression normalized to glyceraldehyde-3-phosphate dehydrogenase (GAPDH) of phosphorylated BAD (pBAD) isoforms (pBAD-155, -136, -112), total BAD, PP2C (PPM1A), phosphorylated PKA (pPKA), and total PKA as measured by Western blot at baseline and after *in vitro* induction of platinum resistance in T8 OVCA cells. **B**, percent expression of pBAD at serine-155, -136, and -112 by immunofluorescence in an independent set of 147 primary advanced-stage OVCA samples, including platinum sensitive/CR ($n = 86$) and platinum resistant/IR ($n = 61$). Error bars indicate SEM.



(A) mutations [BAD(S136A), BAD(S155A)] in BAD (site mutations that prevent phosphorylation of the BAD protein) resulted in increased cisplatin-induced apoptosis compared with cells transfected with wild-type BAD (Fig. 4A). In contrast, cells transfected with BAD(S112A) had no effect on cisplatin sensitivity (Fig. 4A). MTS cell viability analysis (CellTiter96; Promega) showed that cells expressing wild-type, S112A, S136A, and S155A mutations maintained similar proliferation rates after 72 hours of growth.

The role of pBAD (serine-155) in cisplatin sensitivity was further evaluated in A2780S cells by depletion of PKA and PP2C/PPM1A by using siRNA. Depletion of PKA and PP2C/PPM1A resulted in reduced target protein expression (Fig. 4B). Depletion of PKA decreased pBAD levels and increased cisplatin-induced apoptosis compared with cells transfected with a nontargeting control siRNA. In contrast, cells depleted of PP2C/PPM1A showed increased pBAD levels and decreased cisplatin-induced apoptosis (Fig. 4B and C).

A 47-gene BAD-pathway score is associated with *in vitro* phospho-BAD levels and human cancer clinical outcome

On the basis of the above data, we developed a 47-gene BAD-pathway score in the cell line data and evaluated it in

an OVCA genomic data set data (Supplementary Table S3). For cell lines, we identified a negative correlation between BAD-pathway signature score and levels of pBAD (serine-155) protein in cells treated with low-dose cisplatin (schedule A; Pearson score = -0.92 , $P = 0.001$) and higher dose cisplatin (schedule C; Pearson score = -0.72 , $P = 0.045$; Fig. 5A and B). Although pBAD (serine-112 and 136) levels did not show statistically significant correlations with BAD-pathway score, when high and low dosing schedules are evaluated together (schedules A and C), mean BAD pathway score is higher in cells with low versus high levels of pBAD (serine-112) and pBAD (serine-136), using median pBAD as a cutoff (Fig. 5C and D). For the OVCA patient data, the BAD-pathway score was associated with overall survival from OVCA ($n = 142$, $P \leq 0.0001$, Fig. 6A). Furthermore, the OVCA genomic data set was evaluated with regard to BAD-pathway score and surgical cytoreductive (debulking, $n = 141$; debulking status unavailable for 1 of 142 patients) status (optimal: <1 cm; suboptimal: >1 cm residual tumor at conclusion of surgery; $P < 0.0001$; Fig. 6B) and also response to primary platinum-based therapy (CR or IR, $P < 0.0001$, Fig. 6C). The association of high BAD-pathway score and favorable outcome was observed in patients who underwent optimal and

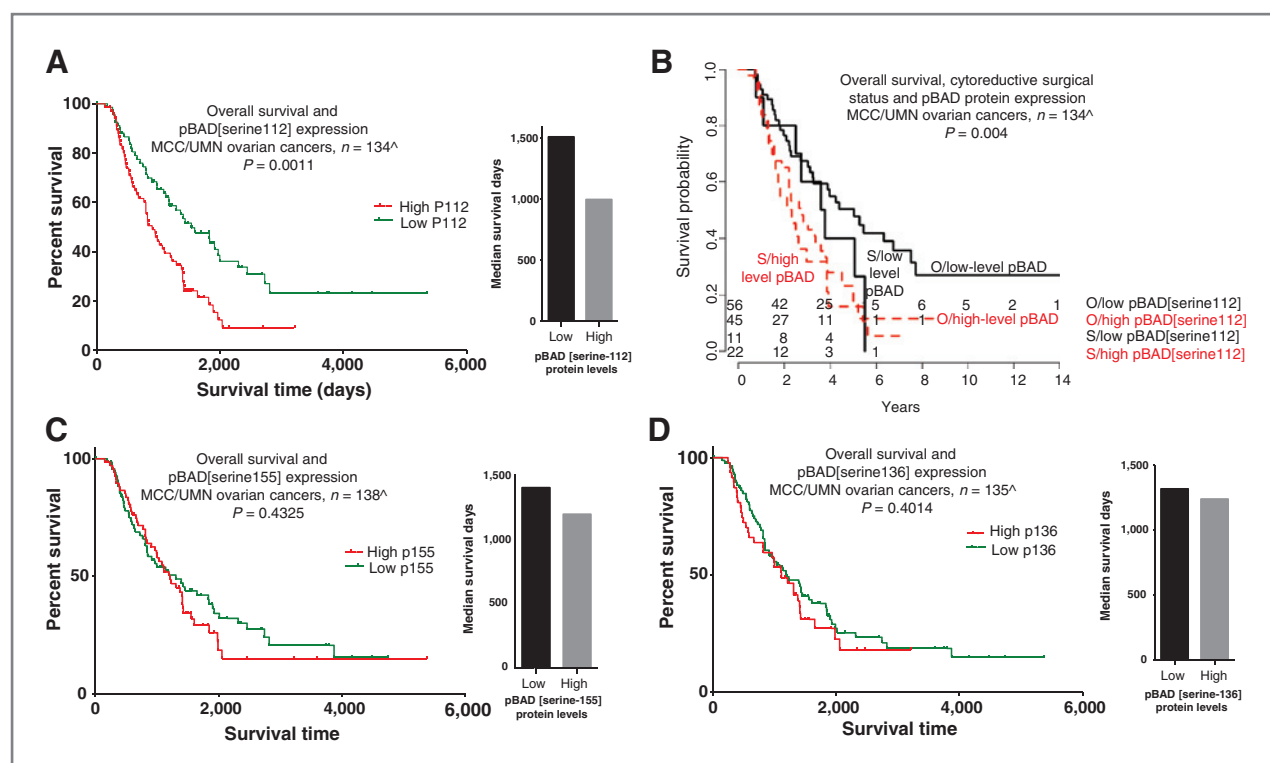


Figure 3. Low expression levels of pBAD protein is associated with overall survival. A, pBAD (serine-112) levels and overall survival, represented by Kaplan-Meier curves (left) and bar graphs for median survival (right). B, Kaplan-Meier overall survival curves for pBAD (serine-112) levels with cytoreductive surgical status. C, pBAD (serine-155) levels and overall survival, represented by Kaplan-Meier curves (left) and bar graphs for median survival (right). D, pBAD (serine-136) levels and overall survival, represented by Kaplan-Meier curves (left) and bar graphs for median survival (right). MCC/UMN, Moffitt Cancer Center and University of Minnesota data sets. [^], information available out of 147 samples. The numbers at risk are shown at bottom of graphs. Log-rank test *P* values indicate significance. O, optimal; S, suboptimal.

suboptimal debulking (optimal: adjusted *P* = 0.007; suboptimal: adjusted *P* = 0.06). Most importantly, OVCA patients with a high BAD-pathway score who underwent suboptimal debulking had a survival that trended toward superiority versus patients with a low BAD-pathway score who underwent optimal debulking (adjusted *P* = 0.19). Similarly, patients who showed an IR to primary platinum-based therapy but had a high BAD-pathway score had no statistical difference in survival compared with those patients who showed a CR but had a low BAD-pathway score (adjusted *P* = 0.22). When evaluated with debulking status and response to primary platinum-based therapy, grade, and age, the Cox proportional hazards model revealed that the BAD-pathway score was an independent variable associated with survival (*P* = 0.01).

Discussion

Few clinical or biologic events affect the outcome for patients with OVCA more than response to chemotherapy. In this study, using a novel *in vitro* strategy, we identified and characterized the BAD apoptosis pathway to be influential in the response of OVCA to chemotherapy, likely via modulation of BAD phosphorylation; we also identified expression of this pathway to be independently

associated with clinical outcome for patients with OVCA. Furthermore, levels of the pBAD protein are not only associated with mRNA expression of the pathway (measured by a 47-gene pathway signature score), but are also independently associated with survival from OVCA. We provide extensive validation of our findings (and the importance of the BAD pathway) with *in vitro* functional studies and *in vivo* and *in silico* analyses of 289 patient specimens and/or data sets. Our findings are further validated by the fact that many of our BAD pathway signature genes, including *RAF1*, *BAD*, *PPM1B*, *PPM1F*, *GNAS*, *PRKAR1A*, *BAX*, *PIK3CD*, and *PTPN11*, have previously been reported to be associated with OVCA chemosensitivity (8, 10, 17–21). Our work builds upon previous reports that suggest that phosphorylation of the BAD protein may be associated with cisplatin resistance in ovarian and head and neck cancer cell lines (22, 23). Interestingly, however, Konstantinopoulos and colleagues recently analyzed 4 microarray data sets including 265 advanced-stage OVCAs and identified and validated a 19-gene prognostic model. Neither the 19-gene model nor the pathways associated with high-risk versus low-risk disease included representation of the BAD pathway (24).

BAD is a member of the BCL2 family of proteins, which are characterized by the presence of up to 4 BCL2-homology

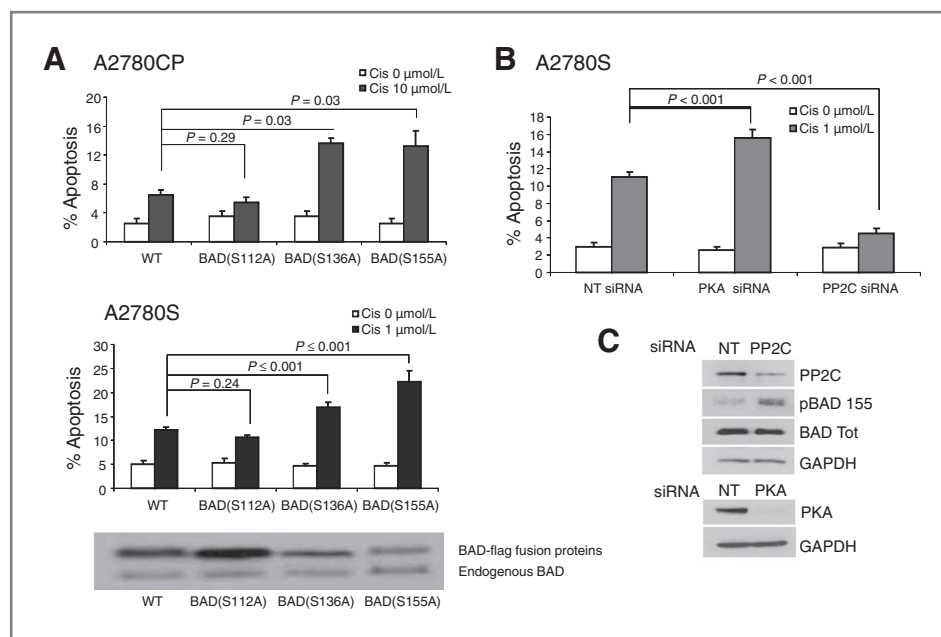


Figure 4. Modulation of BAD protein phosphorylation status influences cisplatin sensitivity. **A**, OVCA cell lines A2780S and A2780CP were transfected with pFlag-600 vectors expressing wild-type BAD (WT) or BAD harboring serine (S) to alanine (A) point mutations in serine-112, -136, or -155 (S112A, S136A, S155A). These S-to-A phosphorylation site mutations prevent phosphorylation of the BAD protein. Transfected cells were treated with vehicle or 1 μmol/L (A2780S) or 10 μmol/L (A2780CP) cisplatin for 48 hours and evaluated for the presence of apoptotic nuclei. **B**, percent apoptotic nuclei in A2780S cells in the presence of 1 μmol/L cisplatin after siRNA depletion of PKA and PP2C. Similar results were observed by 2 different siRNAs for each PP2C and PKA. Error bars indicate SEM. **C**, Western blot showing depletion of PP2C and PKA by siRNA. Controls included a nontargeting siRNA (NT). Glyceraldehyde-3-phosphate dehydrogenase (GAPDH) was used as a loading control.

domains (25). This family includes inhibitors and promoters of apoptosis, such that cell survival versus death is determined by the relative ratio of proapoptotic (e.g., BCL-Xs, BAD, Bax, Bak) and antiapoptotic (e.g., Bcl-2, Bcl-xL, MCL-1, A1, BAG-1) family members (25–28). BAD selectively heterodimerizes with Bcl-xL and Bcl-2 but not with Bax, Bcl-xs, Mcl-1, A1, or itself. When BAD dimerizes with Bcl-xL, Bax is displaced, mitochondrial membrane permeability increases, and apoptosis is induced (29). However, BAD function is regulated by phosphorylation (including serine-112, -136, and -155). When phosphorylated, BAD is unable to heterodimerize with Bcl-2 or Bcl-xL, freeing Bcl-xL to dimerize and functionally sequester Bax, such that it is no longer free to induce apoptosis (29). Thus, the phosphorylation status of BAD determines whether Bax is displaced from Bcl-xL to drive cell death. BAD is thought to be phosphorylated at serine-136 by protein kinase B (PKB/Akt; 30). In contrast, serine-112 is phosphorylated by mitogen-activated protein kinase-activated protein kinase-1 (MAPKAP-K1, also called RSK) and PKA. Serine-155, at the center of the BAD BH3 domain, is phosphorylated preferentially by PKA, which also inhibits Bcl-xL binding (31–33). Conversely, the activity of a series of phosphatases, including PP1, PP2A, and PPM1 (PP2C/PPM1A), as well as calcineurin, has been shown to have proapoptotic effects via dephosphorylation of BAD (34, 35).

Using an *in vitro* model to induce OVCA cisplatin resistance, we have identified expression of BAD apoptosis pathway genes to be associated with the evolution of cisplatin resistance and recognized that many of these genes are kinases or phosphatases that influence the phosphorylation status of the BAD protein. Consistently, we found that pBAD levels increased with OVCA cisplatin resistance in both the cell lines and primary patient samples and that pBAD protein levels were associated with poor overall survival from OVCA. To validate our findings and the importance of the BAD pathway, we showed that *in vitro* manipulation of pBAD levels (by siRNA depletion of a BAD kinase or BAD phosphatase or by targeted mutagenesis of some BAD phosphorylation sites) resulted in a corresponding change in cisplatin-induced apoptosis, without changes to proliferation. To support and further explore the clinical relevance of these findings, we evaluated a 47-gene BAD-pathway score and phospho-BAD in a panel of OVCA cells in which we induced cisplatin resistance by serial treatments and OVCA data/samples obtained from 289 patients. Our results show that a high BAD-pathway signature score is associated with low *in vitro* pBAD levels and favorable overall survival for patients with OVCA. Importantly, analyses of OVCA genomic data and pBAD protein levels from patients with advanced-stage disease have suggested that the influence of the BAD pathway on overall survival may be more important than

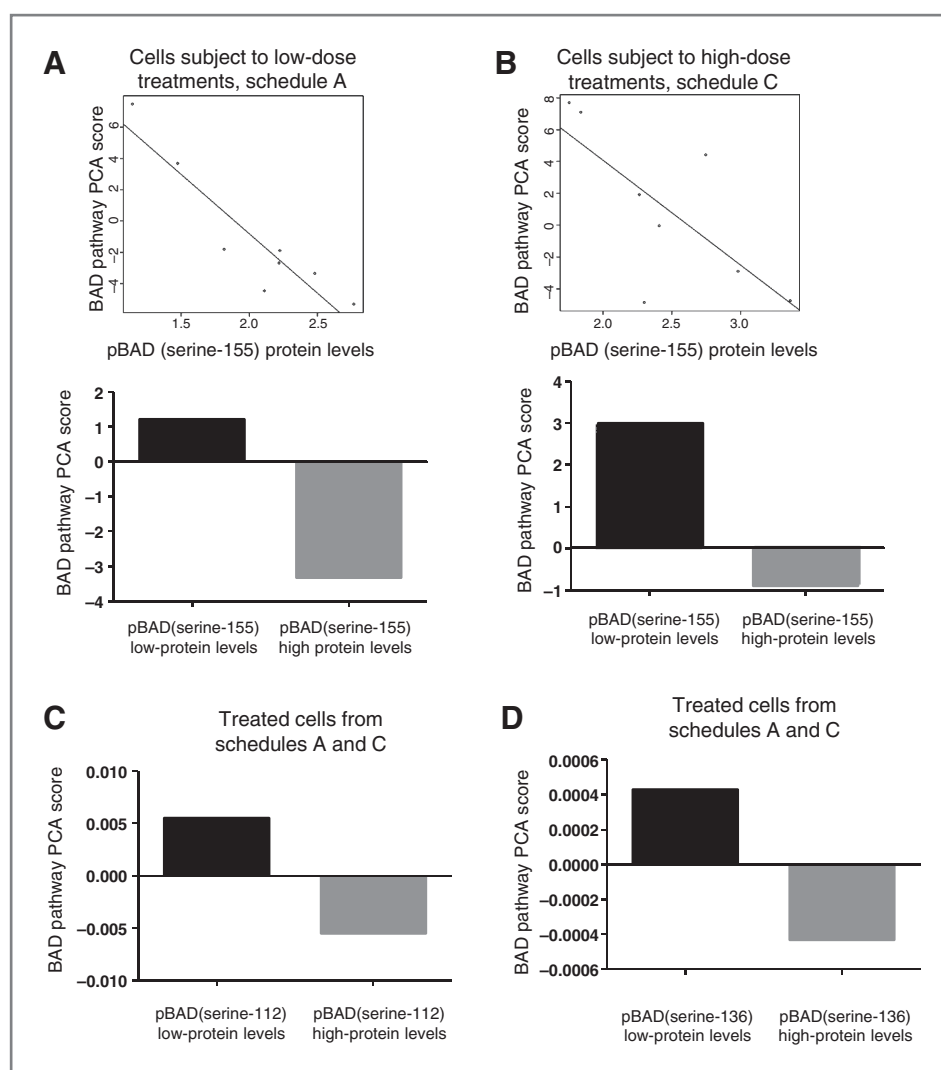


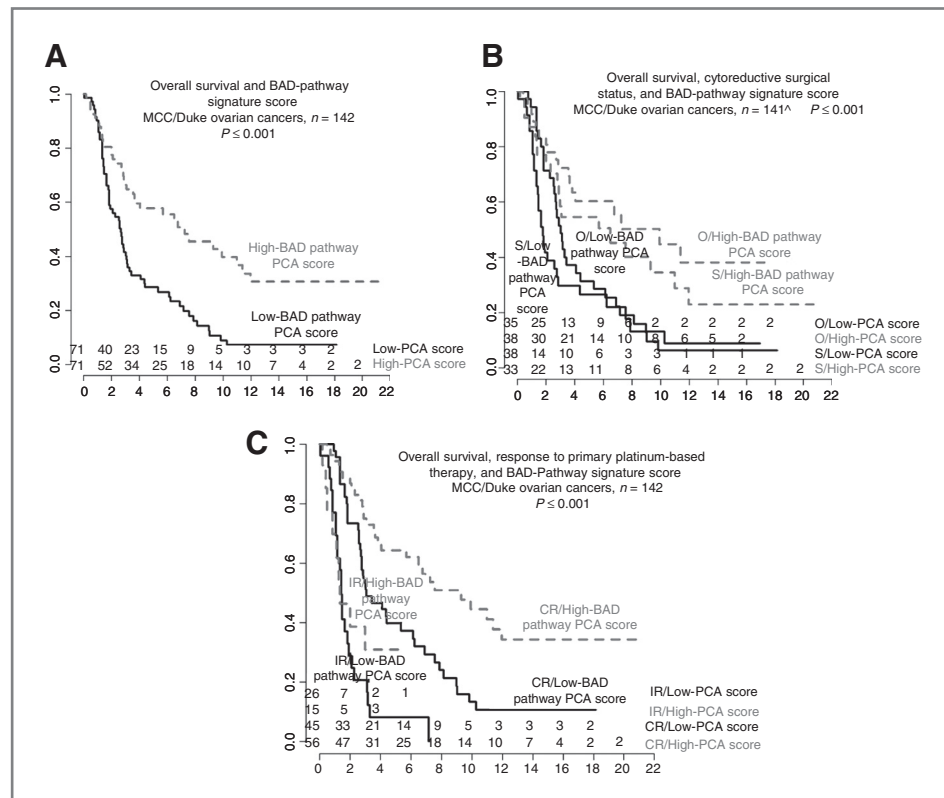
Figure 5. High BAD-pathway signature principal component analysis (PCA) score is associated with low expression levels of pBAD protein. Scatter plots show negative correlation between PCA score and pBAD (serine-155) protein levels and bar graphs show inverse relationship between mean PCA score and pBAD (serine-155) protein levels in cell lines subjected to low-dose (A) treatment schedule A ($P = 0.001$) and high-dose (B) treatment schedule C ($P = 0.045$). Mean PCA score was associated with low pBAD (serine-112; C) and low pBAD (serine-136; D) protein levels in treated cells from combined schedules A and C. For the bar graphs, the appropriate median pBAD (serine-155, -136, or -112) protein levels was used as the cutoff.

the volume of residual disease at the completion of primary surgery, traditionally one of the most important clinical determinants of outcome for patients with OVCA. Such findings could have substantial implications for future clinical treatment of patients with this disease, although additional studies are required. Notably, survival for patients with low versus high levels of phospho-BAD was superior when considering each phosphorylation site (serine-112, -136, -155); however, only the serine-112 site reached statistical significance (Fig. 3). Clearly, additional functional analyses are warranted to better define the mechanistic basis to our observations; our analysis does not speak to the relative importance of each BAD phosphorylation sites or to any potential influence of sequence of BAD phosphorylation on cellular function and clinical outcome. Furthermore, it is worth noting that although our data highlight the importance of this pathway, not all cell lines showed associations between increasing CIS resistance and expression of BAD pathway genes, emphasizing

that OVCA is a highly heterogeneous disease and it is likely that many other pathways and biologic processes contribute to the development of chemoresistance and influence patient survival. In this regard, it is also noteworthy that use of the term "BAD pathway" may be somewhat arbitrary, given the interactions and cross-talk with other closely related proteins and pathways (e.g., RAS-RAF-MEK, PI-3k-AKT, BCL-XL/BAX) many of which have been associated with OVCA drug resistance (36–38).

In addition to characterizing a mechanism by which epithelial OVCAs develop resistance to chemotherapy, we have identified a pathway that has significant clinical relevance as a potential biomarker of therapeutic response and overall patient survival and as a promising therapeutic target. Use of such BAD pathway-based biomarkers could form the basis of an individualized therapeutic approach to women with OVCA, enabling patients to be stratified into high- and low-risk groups, the latter being offered more aggressive therapy, enrollment in clinical trials of novel

Figure 6. High BAD-pathway signature PCA score is associated with favorable clinical outcome. A–C, Kaplan–Meier curves depicting the association between BAD-pathway signature PCA score and overall survival from cancer for MCC and Duke data sets. [^], information available for 141 of 142 samples. The numbers at risk are shown at bottom of graphs. Log-rank test *P* values indicate significance. O, optimal; S, suboptimal.



agents, or the addition of pBAD inhibitors to standard of care drugs.

Disclosure of Potential Conflicts of Interest

No potential conflicts of interest were disclosed. Opinions, interpretations, conclusions, and recommendations are those of the author and are not necessarily endorsed by the funding agencies.

Acknowledgments

We thank Rasa Hamilton (Moffitt Cancer Center) for editorial assistance.

References

- Baker VV. Salvage therapy for recurrent epithelial ovarian cancer. *Hematol Oncol Clin North Am* 2003;17:977–88.
- Hansen HH, Eisenhauer EA, Hansen M, Neijt JP, Piccart MJ, Sessa C, et al. New cytostatic drugs in ovarian cancer. *Ann Oncol* 1993;4 Suppl 4:63–70.
- Herrin VE, Thigpen JT. Chemotherapy for ovarian cancer: current concepts. *Semin Surg Oncol* 1999;17:181–8.
- Godwin AK, Meister A, O'Dwyer PJ, Huang CS, Hamilton TC, Anderson ME. High resistance to cisplatin in human ovarian cancer cell lines is associated with marked increase of glutathione synthesis. *Proc Natl Acad Sci U S A* 1992;89:3070–4.
- Johnson SW, Laub PB, Beesley JS, Ozols RF, Hamilton TC. Increased platinum-DNA damage tolerance is associated with cisplatin resistance and cross-resistance to various chemotherapeutic agents in unrelated human ovarian cancer cell lines. *Cancer Res* 1997;57:850–6.
- Johnson SW, Swiggard PA, Handel LM, Brennan JM, Godwin AK, Ozols RF, et al. Relationship between platinum-DNA adduct formation and removal and cisplatin cytotoxicity in cisplatin-sensitive

Grant Support

This project was supported in part by National Cancer Institute Grant R21 CA-110499-01A2, the Ocala Royal Dames For Cancer Research Inc., the Phi Beta Psi Sorority, the Hearing the Ovarian Cancer Whisper, Jacquie Liggett Foundation, the Ovarian Cancer Research Fund, and the US Army Medical Research and Materiel Command under Award No. DAMD17-02-2-0051.

The costs of publication of this article were defrayed in part by the payment of page charges. This article must therefore be hereby marked *advertisement* in accordance with 18 U.S.C. Section 1734 solely to indicate this fact.

Received March 18, 2011; revised July 8, 2011; accepted August 1, 2011; published OnlineFirst August 17, 2011.

- and -resistant human ovarian cancer cells. *Cancer Res* 1994;54:5911–6.
- Benedetti V, Perego P, Luca Beretta G, Corna E, Tinelli S, Righetti SC, et al. Modulation of survival pathways in ovarian carcinoma cell lines resistant to platinum compounds. *Mol Cancer Ther* 2008;7:679–87.
- Dressman HK, Berchuck A, Chan G, Zhai J, Bild A, Sayer R, et al. An integrated genomic-based approach to individualized treatment of patients with advanced-stage ovarian cancer. *J Clin Oncol* 2007;25:517–25.
- Jazaeri AA, Awtry CS, Chandramouli GV, Chuang YE, Khan J, Sotiriou C, et al. Gene expression profiles associated with response to chemotherapy in epithelial ovarian cancers. *Clin Cancer Res* 2005;11:6300–10.
- Boren T, Xiong Y, Hakam A, Wenham R, Apte S, Chan G, et al. MicroRNAs and their target messenger RNAs associated with ovarian cancer response to chemotherapy. *Gynecol Oncol* 2009;113:249–55.
- Bild AH, Yao G, Chang JT, Wang Q, Potti A, Chasse D, et al. Oncogenic pathway signatures in human cancers as a guide to targeted therapies. *Nature* 2006;439:353–7.

12. Irizarry RA, Hobbs B, Collin F, Beazer-Barclay YD, Antonellis KJ, Scherf U, et al. Exploration, normalization, and summaries of high density oligonucleotide array probe level data. *Biostatistics* 2003;4:249–64.
13. Bolstad BM, Irizarry RA, Astrand M, Speed TP. A comparison of normalization methods for high density oligonucleotide array data based on variance and bias. *Bioinformatics* 2003;19:185–93.
14. Chen N, Kamath S, Newcomb J, Hudson J, Garbuzova-Davis S, Bickford P, et al. Trophic factor induction of human umbilical cord blood cells *in vitro* and *in vivo*. *J Neural Eng* 2007;4:130–45.
15. Marchion DC, Bicaku E, Turner JG, Daud AI, Sullivan DM, Munster PN. Synergistic interaction between histone deacetylase and topoisomerase II inhibitors is mediated through topoisomerase IIbeta. *Clin Cancer Res* 2005;11:8467–75.
16. Holm S. A simple sequentially rejective multiple test procedure. *Scand J Statist* 1979;6:65–70.
17. Britten RA, Perdue S, Eshpeter A, Merriam D. Raf-1 kinase activity predicts for paclitaxel resistance in TP53mut, but not TP53wt human ovarian cancer cells. *Oncol Rep* 2000;7:821–5.
18. Cvijic ME, Chin KV. Effects of R1alpha overexpression on cisplatin sensitivity in human ovarian carcinoma cells. *Biochem Biophys Res Commun* 1998;249:723–7.
19. Helleman J, Jansen MP, Span PN, van Staveren IL, Massuger LF, Meijer-van Gelder ME, et al. Molecular profiling of platinum resistant ovarian cancer. *Int J Cancer* 2006;118:1963–71.
20. Perego P, Giarola M, Righetti SC, Supino R, Caserini C, Delia D, et al. Association between cisplatin resistance and mutation of p53 gene and reduced bax expression in ovarian carcinoma cell systems. *Cancer Res* 1996;56:556–62.
21. Zhu QY, Wang Z, Ji C, Cheng L, Yang YL, Ren J, et al. C6-ceramide synergistically potentiates the anti-tumor effects of histone deacetylase inhibitors via AKT dephosphorylation and alpha-tubulin hyperacetylation both *in vitro* and *in vivo*. *Cell Death Dis* 2011;2:e117.
22. Do NY, Lim SC. A low level of nicotine-induced chemoresistance in a KB cell line. *Mol Med Report* 2008;1:55–60.
23. Hayakawa J, Ohmichi M, Kurachi H, Kanda Y, Hisamoto K, Nishio Y, et al. Inhibition of BAD phosphorylation either at serine 112 via extracellular signal-regulated protein kinase cascade or at serine 136 via Akt cascade sensitizes human ovarian cancer cells to cisplatin. *Cancer Res* 2000;60:5988–94.
24. Konstantinopoulos PA, Cannistra SA, Fountzilas H, Culhane A, Pillay K, Rueda B, et al. Integrated analysis of multiple microarray datasets identifies a reproducible survival predictor in ovarian cancer. *PLoS One* 2011;6:e18202.
25. Danial NN, Korsmeyer SJ. Cell death: critical control points. *Cell* 2004;116:205–19.
26. Dejean LM, Martinez-Caballero S, Guo L, Hughes C, Teijido O, Ducret T, et al. Oligomeric Bax is a component of the putative cytochrome c release channel MAC, mitochondrial apoptosis-induced channel. *Mol Biol Cell* 2005;16:2424–32.
27. Desagher S, Osen-Sand A, Nichols A, Eskes R, Montessuit S, Lauper S, et al. Bid-induced conformational change of Bax is responsible for mitochondrial cytochrome c release during apoptosis. *J Cell Biol* 1999;144:891–901.
28. Kuwana T, Mackey MR, Perkins G, Ellisman MH, Latterich M, Schneider R, et al. Bid, Bax, and lipids cooperate to form supramolecular openings in the outer mitochondrial membrane. *Cell* 2002;111:331–42.
29. Yang E, Zha J, Jockel J, Boise LH, Thompson CB, Korsmeyer SJ. Bad, a heterodimeric partner for Bcl-XL and Bcl-2, displaces Bax and promotes cell death. *Cell* 1995;80:285–91.
30. del Peso L, Gonzalez-Garcia M, Page C, Herrera R, Nunez G. Interleukin-3-induced phosphorylation of BAD through the protein kinase Akt. *Science* 1997;278:687–9.
31. Lizcano JM, Morrice N, Cohen P. Regulation of BAD by cAMP-dependent protein kinase is mediated via phosphorylation of a novel site, Ser155. *Biochem J* 2000;349:547–57.
32. Tan Y, Demeter MR, Ruan H, Comb MJ. BAD Ser-155 phosphorylation regulates BAD/Bcl-XL interaction and cell survival. *J Biol Chem* 2000;275:25865–9.
33. Zhou XM, Liu Y, Payne G, Lutz RJ, Chittenden T. Growth factors inactivate the cell death promoter BAD by phosphorylation of its BH3 domain on Ser155. *J Biol Chem* 2000;275:25046–51.
34. Klumpp S, Selke D, Krieglstein J. Protein phosphatase type 2C dephosphorylates BAD. *Neurochem Int* 2003;42:555–60.
35. Yang L, Omori K, Suzukawa J, Inagaki C. Calcineurin-mediated BAD Ser155 dephosphorylation in ammonia-induced apoptosis of cultured rat hippocampal neurons. *Neurosci Lett* 2004;357:73–5.
36. Castino R, Peracchio C, Salini A, Nicotra G, Trinchieri NF, Demoz M, et al. Chemotherapy drug response in ovarian cancer cells strictly depends on a cathepsin D-Bax activation loop. *J Cell Mol Med* 2009;13:1096–109.
37. Hsu CY, Bristow R, Cha MS, Wang BG, Ho CL, Kurman RJ, et al. Characterization of active mitogen-activated protein kinase in ovarian serous carcinomas. *Clin Cancer Res* 2004;10:6432–6.
38. Peng DJ, Wang J, Zhou JY, Wu GS. Role of the Akt/mTOR survival pathway in cisplatin resistance in ovarian cancer cells. *Biochem Biophys Res Commun* 2010;394:600–5.